Sorting of an Internalized Plasma Membrane Lipid between Recycling and Degradative Pathways in Normal and Niemann-Pick, Type A Fibroblasts

Michael Koval and Richard E. Pagano

Carnegie Institution of Washington, Department of Embryology, Baltimore, Maryland 21210

Abstract. We examined the metabolism and intracellular transport of a fluorescent sphingomyelin analogue, *N*-(*N*-[6-[(7-nitrobenz-2-oxa-1,3-diazol-4-yl)amino]caproyl])-sphingosylphosphorylcholine (C_6-NBD-SM), in both normal and Niemann-Pick, type A (NP-A) human skin fibroblast monolayers. C_6-NBD-SM was integrated into the plasma membrane bilayer by transfer of C_6-NBD-SM monomers from liposomes to cells at 7°C. The cells were washed, and within 3 min of warming to 37°C, both normal and NP-A fibroblasts had internalized C_6-NBD-SM from the plasma membrane, resulting in a punctate pattern of intracellular fluorescence. Rates for C_6-NBD-SM internalization and transport from intracellular compartments to the plasma membrane (recycling) were similar for normal and NP-A cells.

With increasing time at 37°C, internalized C_6-NBD-SM accumulated in the lysosomes of NP-A fibroblasts, while normal fibroblasts showed increasing Golgi apparatus fluorescence with no observable lysosomal labeling. Since NP-A fibroblasts lack lysosomal (acid) sphingomyelinase (A-SMase), this result suggested that hydrolysis of C_6-NBD-SM prevented its accumulation in the lysosomes of normal fibroblasts during its transport along the degradative pathway.

We used the amount of C_6-NBD-SM hydrolysis by A-SMase in normal cells as a measure of C_6-NBD-SM transported from the cell surface to the lysosomes. After a lag period, C_6-NBD-SM was delivered to the lysosomes at a rate of ~8%/h. This rate was ~18–19fold slower than the rate of C_6-NBD-SM recycling from intracellular compartments to the plasma membrane. Thus, small amounts of C_6-NBD-SM were transported along the degradative pathway, while most endocytosed C_6-NBD-SM was sorted for transport along the plasma membrane recycling pathway.

RECEPTORS internalized from the plasma membrane are generally either recycled back to the plasma membrane or are transported along the "degradative" pathway to the lysosomes (reviewed in Goldstein et al., 1985; Wileman et al., 1985; Hubbard, 1989). An acidic intracellular compartment, known as sorting endosomes, 'early' endosomes, or CURL (compartment of uncoupling of receptor and ligand), has been implicated in the targeting of receptors to the appropriate destination (Geuze et al., 1983, 1987). One model for receptor sorting is that vesicles formed from tubular extensions of the sorting endosome are preferentially sorted to the plasma membrane. The remainder of the sorting endosome membrane, including most of the lumenal volume, moves to the lysosomal compartment (Rome, 1985; Linderman and Lauffenburger, 1988; Dunn et al., 1989).

One prediction of this model is that lipids internalized from the plasma membrane (Fig. 1, pathway *I*) should be transported through a sorting compartment to both the recycling pathway (Fig. 1, pathway *II*) and degradative pathway (Fig. 1, pathway *III*), provided that lipids are free to diffuse throughout the sorting endosome membrane. Further, if plasma membrane recycling is the major pathway for bulk flow of endocytosed membrane, one would expect that most of the endocytosed lipid would be returned to the plasma membrane.

Previously, we examined the transport of C_6-NBD-SM in CHO-K1 fibroblasts and found that the fluorescent lipid was recycled between intracellular compartments and the plasma membrane (Koval and Pagano, 1989). Both C_6-NBD-SM and Rh-transferrin, a protein that recycles, showed similar intracellular distributions upon internalization in CHO-K1 cells, suggesting that endocytosed C_6-NBD-SM is transported to sorting endosomes in these cells.

Although we measured C_6-NBD-SM recycling in CHO cells (i.e., Fig. 1, pathways *I* and *II*), C_6-NBD-SM did not label the lysosomes of these cells. One possibility is that C_6-NBD-SM recycling is dominant and the levels of C_6-

M. Koval's present address is Washington University School of Medicine, Department of Cell Biology and Physiology, St. Louis, MO 63110.

This work is in partial fulfillment of the requirements for a doctoral degree by M. Koval in the Department of Biology, The Johns Hopkins University, Baltimore, MD.

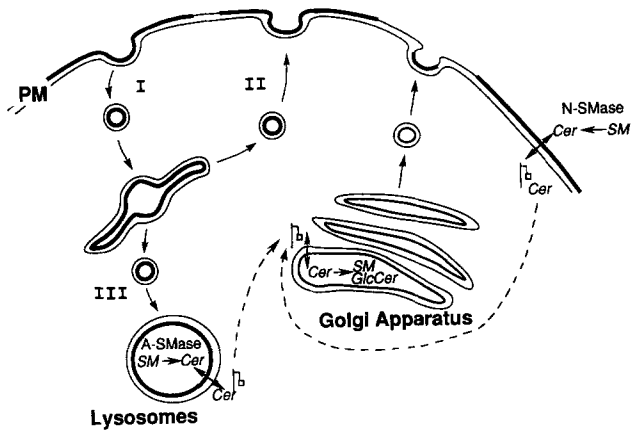

Figure 1. Model for C_6-NBD-SM transport and metabolism in human skin fibroblasts. Thick lines represent portions of the bilayer containing fluorescent lipid. Nonmetabolized C_6-NBD-SM inserted into the outer leaflet of the plasma membrane (*PM*) is endocytosed (pathway *I*) to a compartment where it is sorted between pathway II, resulting in PM lipid recycling, and pathway III, a degradative pathway leading to lysosomes. Endogenous SM hydrolysis is presumed to occur either at the PM, by N-SMase (both normal and NP-A fibroblasts), and at the lysosomes by A-SMase (normal fibroblasts only). After C_6-NBD-SM hydrolysis, the fluorescent Cer produced can undergo transbilayer movement ("flip-flop") and subsequent transport to the Golgi apparatus (*broken lines*) where C_6-NBD-Cer is metabolized to newly synthesized C_6-NBD-SM and C_6-NBD-GlcCer (see text).

NBD-SM transported along the degradative pathway (Fig. 1, pathway *III*) are too small to be detected. Alternatively, C_6-NBD-SM might be transported to lysosomes but not retained there. For example, rapid retrograde transport of lipid from lysosomes to endosomes might occur. Alternatively, any fluorescent SM delivered to lysosomes might be rapidly hydrolyzed there to form C_6-NBD-Cer. Since C_6-NBD-Cer can undergo transbilayer movement (Pagano, 1989) and is capable of rapid and spontaneous monomeric diffusion (Pagano and Martin, 1988; Pagano, 1989), conversion of C_6-NBD-SM to C_6-NBD-Cer would permit rapid transport of C_6-NBD-lipid from the lysosomes to other intracellular membranes (Fig. 1, *broken lines*). In particular, the Golgi apparatus has a high affinity for C_6-NBD-Cer (Lipsky and Pagano, 1985*b*; Pagano and Martin, 1988; Pagano et al., 1989; Pagano, 1990). Consistent with this model, CHO-K1 cells labeled with C_6-NBD-SM and then incubated at 37°C, hydrolyze increasing amounts of C_6-NBD-SM with time and show concomitant increases in Golgi apparatus fluorescence (Koval and Pagano, 1989).

If hydrolysis of C_6-NBD-SM is required for rapid depletion of C_6-NBD-lipid from lysosomes, then elimination of A-SMase should result in accumulation of fluorescent SM in the lysosomes. Niemann-Pick, type A (NP-A) fibroblasts are deficient in A-SMase (Beaudet and Manschreck, 1982; Maziere et al., 1982). Differences in SM metabolism between normal and NP-A fibroblasts have previously been examined using exogenously added radiolabeled SM (Kudoh et al., 1983; Sutrina and Chen, 1984) and fluorescent (pyrene) SM (Levade and Gatt, 1987). Also, radiolabeling of endogenous SM, through the use of labeled metabolic precursors, has been used to measure SM hydrolysis and turnover in NP-A fibroblasts (Spence et al., 1983). Most studies on SM metabolism in NP-A fibroblasts focus on the long-term metabolism of SM (hours to days), and thus are difficult to interpret in the context of vesicular transport of SM between intracellular compartments, which occurs at rates of minutes to hours.

In this study, we examined normal and NP-A fibroblasts labeled at the plasma membrane with C_6-NBD-SM and used fluorescence microscopy to demonstrate that the mutant fibroblasts accumulated endocytosed C_6-NBD-SM in the lysosomes. This suggested that normal cells also transported C_6-NBD-SM to the lysosomes. Since any C_6-NBD-SM transported to the lysosomes in normal cells is likely to be rapidly hydrolyzed, the amount of C_6-NBD-SM hydrolyzed by A-SMase should correspond to the amount of C_6-NBD-SM transported along the degradative pathway. We were able to confirm this hypothesis, determine the amount of C_6-NBD-SM transported to the lysosomes, and by comparison to the rate for C_6-NBD-SM returned to the plasma membrane, determine the relative amount of C_6-NBD-SM sorted along these two pathways.

Glossary

A-SMase	acid sphingomyelinase
C_6-NBD-	*N*-[6-[(7-nitrobenz-2-oxa-1,3-diazol-4-yl)amino]caproyl]
C_6-NBD-Cer	*N*-(C_6-NBD)-sphingosine
C_6-NBD-GlcCer	*N*-(C_6-NBD)-glucosylsphingosine
C_6-NBD-SM	*N*-(C_6-NBD)-sphingosylphosphorylcholine
Cer	ceramide
CHO-K1	Chinese hamster ovary fibroblast cell line
DOPC	dioleoylphosphatidylcholine
GlcCer	glucosylceramide
HCMF	10 mM Hepes-buffered calcium and magnesium-free Puck's saline, pH 7.4
hLAMP	human lysosome-associated membrane protein
HMEM	Hepes-buffered MEM
N-SMase	neutral sphingomyelinase
NP-A	Niemann-Pick disease, type A
SM	sphingomyelin
SRh	sulforhodamine
SUV	small unilamellar vesicle

Materials and Methods

Materials

Dioleoylphosphatidylcholine (DOPC) and dioleoylphosphatidylethanolamine were obtained from Avanti Polar Lipids, Inc. (Birmingham, AL). C_6-NBD-fatty acid, Lucifer Yellow, sulforhodamine chloride, and sulforhodamine dextran, molecular mass 10 kD (SRh-dextran) were purchased from Molecular Probes Inc. (Eugene, OR). Sodium cacodylate was from Electron Microscopy Sciences (Fort Washington, PA). All organic solvents were purchased from Burdick & Jackson Laboratories Inc. (Muskegon, MI). Fluorescein-conjugated second antibodies were from Organon Teknika-Cappel (Malvern, PA). Unless otherwise stated, all other materials were obtained from Sigma Chemical Co. (St. Louis, MO).

Cell Culture

Monolayer cultures of normal (No. GM41) and Niemann-Pick, type A (No. GM112) fibroblasts were obtained from the Coriell Institute for Medical Research (Camden, NJ) and grown in DME (No. 430-2100; Gibco Laboratories, Grand Island, NY) supplemented with 10% fetal bovine serum (HyClone Laboratories, Logan, UT) in a water-saturated atmosphere of 5% CO_2 in air. Cells were grown for 2–7 d on No. 1 thickness, 25-mm acid-washed glass coverslips to 20% confluency for microscopy, or on 100-mm plastic tissue culture dishes to 80% confluency for biochemical analysis. All cells were between passage numbers 12 and 20.

Lipid Synthesis and Analysis

D-*erythro*-C_6-NBD-SM was synthesized from C_6-NBD-fatty acid and sphingosylphosphorylcholine as described (Koval and Pagano, 1989). *N*-Sulforhodamine-conjugated dioleoylphosphatidylethanolamine (*N*-SRh-DOPE; Uster and Pagano, 1986) and *N*-(C_6-NBD)-D-*erythro*-sphingosine (C_6-NBD-Cer; Pagano and Martin, 1988) were synthesized and purified as described. Concentrations of lipid stock solutions were determined by phosphorus measurement (Rouser et al., 1966) or by reference to known concentrations of fluorescent standards.

Lipid Vesicles

Small unilamellar vesicles (SUV) consisting of either C_6-NBD-SM:DOPC or C_6-NBD-Cer:DOPC (2:3; mol/mol) were formed by ethanol injection (Kremer et al., 1977) as described (Koval and Pagano, 1989) and were typically diluted to a final working concentration of 25 μM total lipid in Hepes-buffered Eagle's MEM, pH 7.4 (HMEM), unless otherwise specified. DOPC vesicles for the back-exchange procedure (see below) were prepared as large unilamellar vesicles by extrusion (LUVET; Hope et al., 1985) and diluted to a final working concentration of 400 μM DOPC in HMEM, as described (Koval and Pagano, 1989).

Incubation of Lipid Vesicles with Cells

Monolayer cultures were cooled to 7°C for 5 min, washed twice with HMEM, and then incubated with vesicles containing fluorescent lipid, usually 25 μM C_6-NBD-SM:DOPC (2:3; mol/mol) SUV in HMEM at 7°C for 30 min. Incubations were stopped by washing the cells three times with cold HMEM. In most experiments, the cultures were subsequently warmed to 37°C by adding prewarmed HMEM to the cells and incubating at 37°C in a water bath.

To remove C_6-NBD-SM associated with the plasma membrane, the cells were back-exchanged (Sleight and Pagano, 1984; Struck and Pagano, 1980) at 7°C as described (Koval and Pagano, 1989). After back-exchange, cultures sometimes were further incubated at 37°C with either prewarmed HMEM alone or prewarmed HMEM containing LUVETs (back-exchange

Table I. Insertion of C_6-NBD-SM into the Plasma Membrane

Cell type	C_6-NBD-SM/ cell DNA	Cell phospholipid/ cell DNA	C_6-NBD-SM/ cell phospholipid
	pmol/μg	*nmol/μg*	*pmol/nmol*
Normal	93.0 ± 12.3	3.70 ± 0.73	25.1 ± 6.0
NP-A	95.3 ± 10.8	6.20 ± 0.72	15.4 ± 2.5

Both normal and NP-A fibroblasts were incubated with SUV containing C_6-NBD-SM for 30 min at 7°C, washed, and the amount of specific incorporation of C_6-NBD-SM was determined. Also, the total cellular phospholipid per microgram DNA was determined for both cell types. Values are the means of triplicate measurements ± SD.

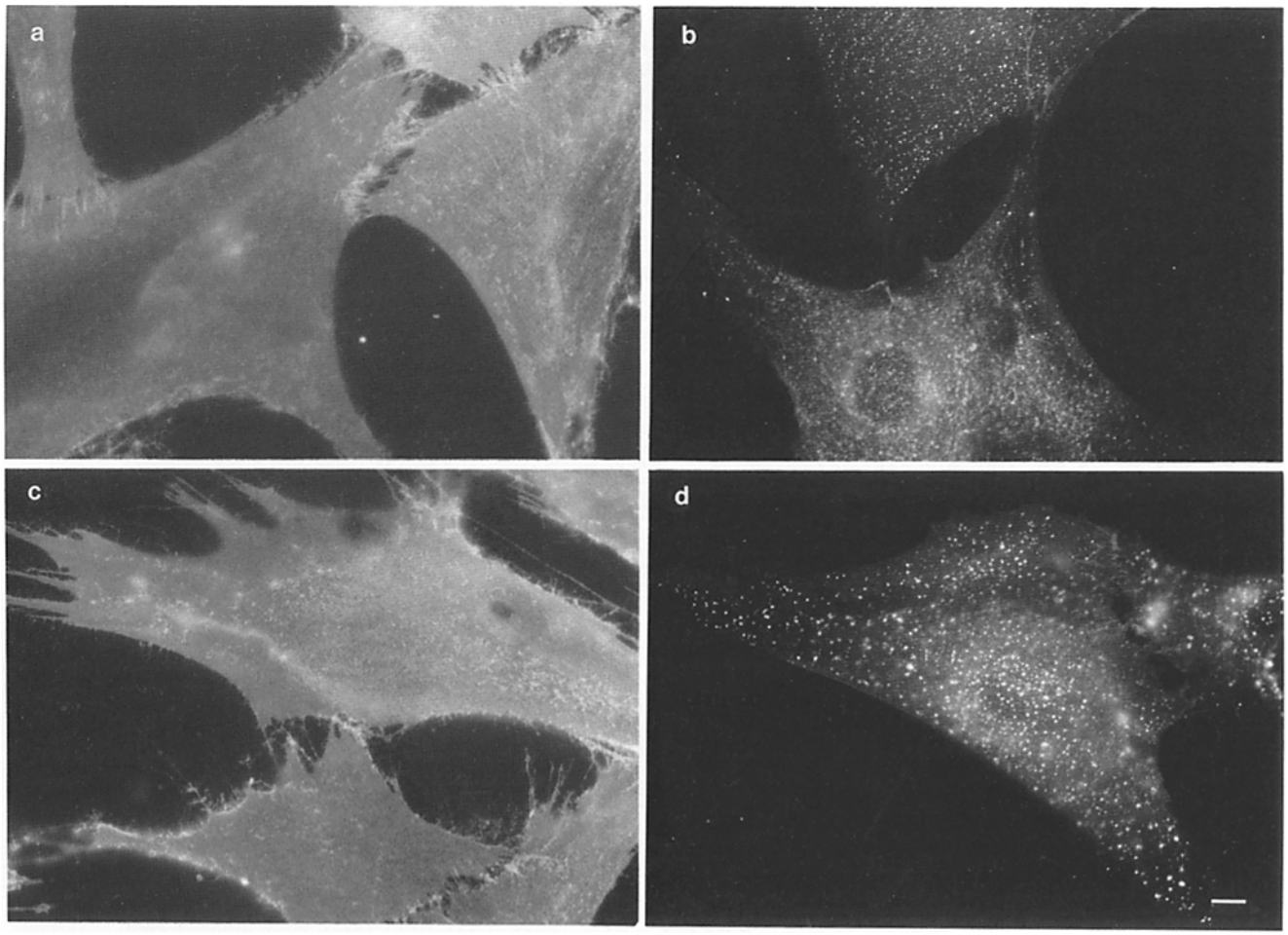

Figure 2. Appearance of C_6-NBD-SM labeling and uptake in human fibroblasts. (*a* and *c*) Normal (*a*) or NP-A (*c*) human fibroblasts were labeled with C_6-NBD-SM/DOPC (2:3; mol/mol) SUV at 25 μM total lipid concentration for 30 min at 7°C, washed, and photographed. (*b* and *d*) Both normal (*b*) and NP-A (*d*) human fibroblasts were labeled as in *a*, washed, incubated for 10 min at 37°C in HMEM, treated with back-exchange medium at 7°C to remove C_6-NBD-SM remaining at the plasma membrane, washed, and photographed. Note the similarity between normal and NP-A fibroblasts treated under these conditions. Bar, 10 μm.

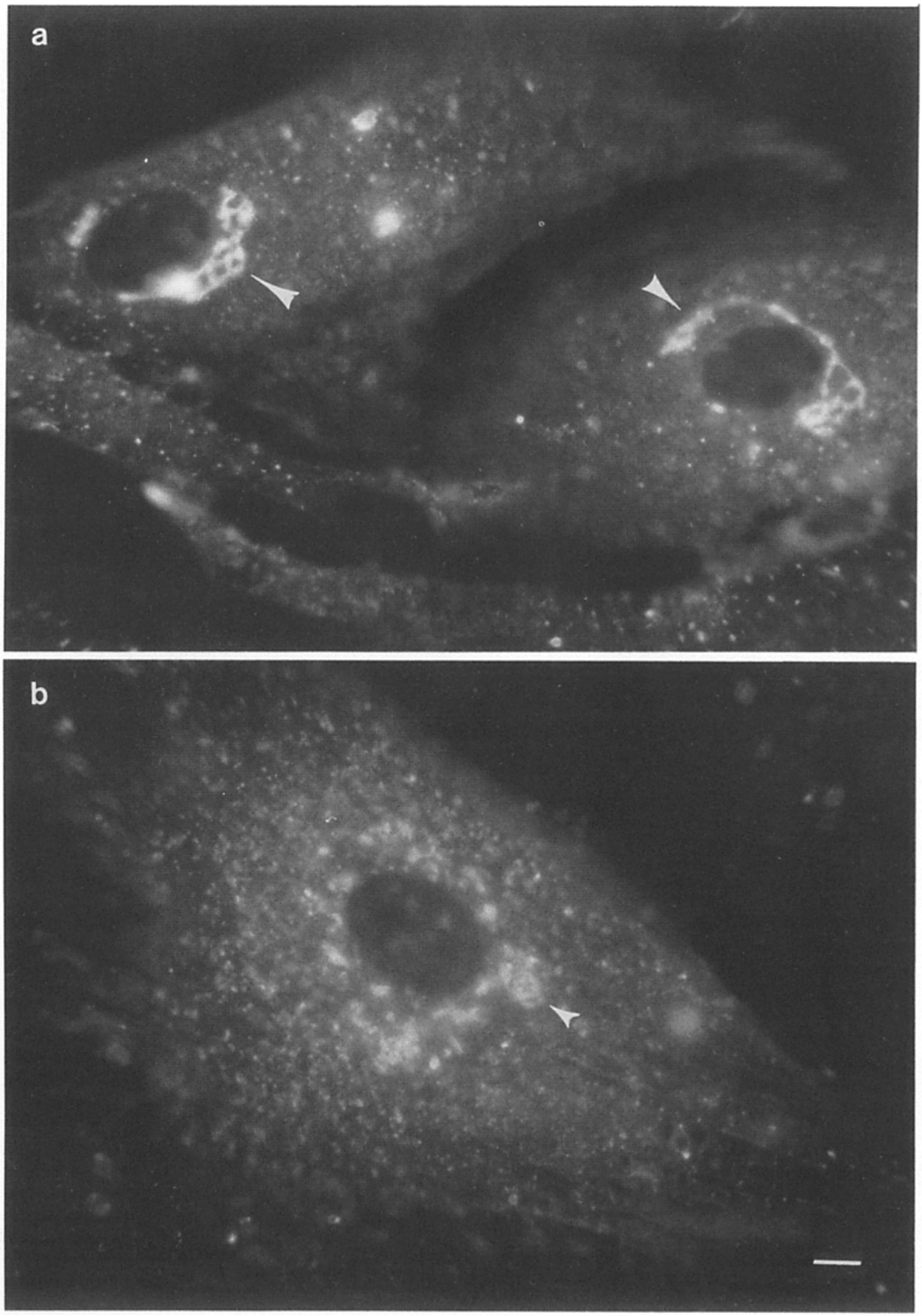

Figure 3. Transport of C_6-NBD-lipid to the Golgi apparatus in normal fibroblasts. Normal (*a*) and NP-A (*b*) human fibroblasts were labeled with SUV containing C_6-NBD-SM for 30 min at 7°C, washed, and incubated in HMEM for 60 min at 37°C. The cells were then treated with back-exchange medium at 7°C to remove C_6-NBD-SM remaining at the plasma membrane, washed, and photographed for C_6-NBD-lipid fluorescence. Although NP-A cells treated in this manner showed some perinuclear fluorescence (*arrowheads*), they did not show the same distinct reticular Golgi apparatus appearance exhibited by normal fibroblasts (*a*). Bar, 10 μm.

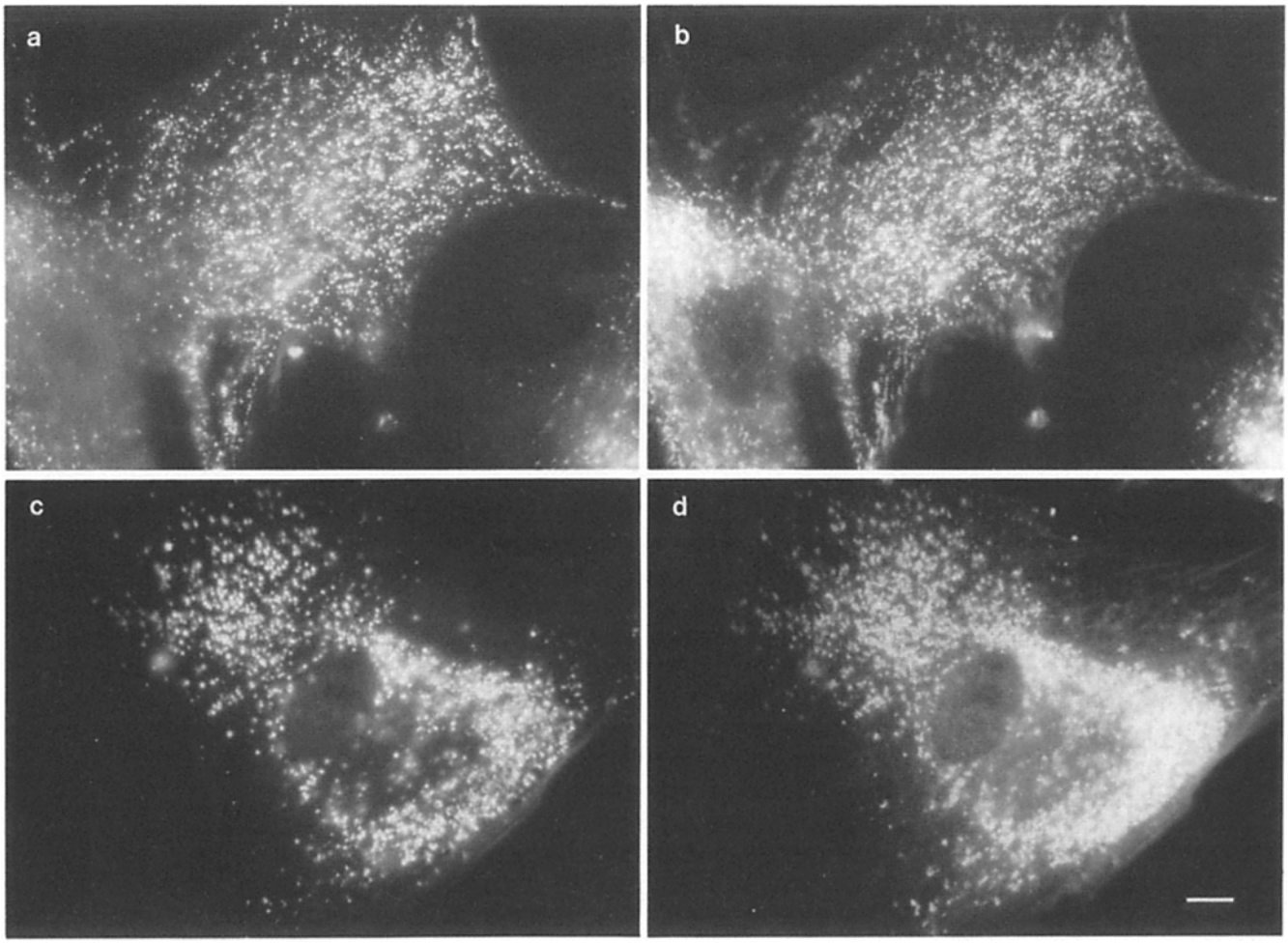

Figure 4. Distribution of lysosomes in human fibroblasts. Normal (*a* and *b*) or NP-A (*c* and *d*) human fibroblasts were incubated overnight in culture medium containing 0.6 μg SRh-dextran/ml, washed, incubated in HMEM for 2 h at 37°C, fixed, and photographed for SRh-dextran fluorescence (*a* and *c*). The cells were subsequently rendered permeable, treated with an antibody to a human lysosome-associated glycoprotein (hLAMP2), washed, labeled with fluorescein-conjugated goat anti-rabbit IgG, washed, and the field previously photographed for SRh fluorescence was rephotographed for fluorescein fluorescence (*b* and *d*). SRh-dextran and hLAMP were found to extensively colocalize. However, since this method required relocation of cells after indirect immunofluorescence labeling, subtle differences in fluorescein and SRh-fluorescence patterns are likely to arise from changes in the plane of focus. Bar, 10 μm.

medium), which removes any C_6-NBD-lipid transported to the plasma membrane during the second 37°C incubation.

To investigate metabolism of C_6-NBD-Cer, cells were labeled for 30 min at 7°C with C_6-NBD-Cer/DOPC (2:3; mol/mol) SUV at (*a*) concentrations of 3–50 μM total lipid, washed, and then incubated for 30 min at 37°C, or (*b*) at 25 μM total lipid, washed, and then incubated at 37°C for times ranging from 5 min to 2 h.

Analysis of Fluorescent Lipid Metabolism

Measurement of cell-associated C_6-NBD-lipid species was determined as described (Koval and Pagano, 1989) by quantitative video imaging of lipid extracts (Bligh and Dyer, 1959) chromatographed on Silica Gel 60 thin-layer plates using $CHCl_3/CH_3OH/28\%$ NH_4OH/H_2O (72:48:2:9; vol/vol/vol/vol) as the developing solvent. DNA content from aliquots of cell samples was determined with Hoescht 33258,(Labarca and Paigen, 1980) using salmon sperm DNA as a standard.

The percentage of C_6-NBD-SM removed by the back-exchange process [% $(C_6\text{-NBD-SM})_{rem}$] was calculated using the equation:

$$\%\ (C_6\text{-NBD-SM})_{rem} = [1 - ((C_6\text{-NBD-SM})_{BX}/(C_6\text{-NBD-SM})_{tot})] \times 100, \quad (1)$$

where the amount of C_6-NBD-SM was determined as pmol fluorescent SM/μg DNA in both back-exchanged cells [$(C_6\text{-NBD-SM})_{BX}$] and non-back-exchanged cells [$(C_6\text{-NBD-SM})_{tot}$]. Back-exchange efficiency was determined by calculating the % $(C_6\text{-NBD-SM})_{rem}$, expressed as a fraction, for cells labeled, maintained at 7°C, and treated with back-exchange medium at 7°C as described (Koval and Pagano, 1989). The amount of C_6-NBD-lipid removed by back-exchange divided by the back-exchange efficiency (normal: 0.90; NP-A: 0.91) reflects the amount of fluorescent lipid located at the plasma membrane (Martin and Pagano, 1987; van Meer et al., 1987; Koval and Pagano, 1989).

The amount of newly-synthesized C_6-NBD-SM in D-*erythro*-C_6-NBD-SM labeled cells was calculated from the amount of cell-associated C_6-NBD-GlcCer by:

$$(\text{newly-synthesized } C_6\text{-NBD-SM}) = R \times (C_6\text{-NBD-GlcCer}), \quad (2)$$

where R was the ratio of C_6-NBD-SM to C_6-NBD-GlcCer synthesized by fibroblasts after incubation with C_6-NBD-Cer [normal: $R = 1.29 \pm 0.14$ (37°C; $n = 18$), 0.73 ± 0.17 (19°C; $n = 7$); NP-A: $R = 0.72 \pm 0.32$ (37°C; $n = 19$), 0.26 ± 0.01 (19°C; $n = 6$)]. The amount of C_6-NBD-SM that was not metabolized was determined by:

$$(\text{nonmetabolized } C_6\text{-NBD-SM}) = (\text{total } C_6\text{-NBD-SM}) - (\text{newly synthesized } C_6\text{-NBD-SM}) \quad (3)$$

Values in Eqs. 2 and 3 were determined as pmol C_6-NBD-SM/μg DNA.

In Vitro Sphingomyelinase Assay

Determination of sphingomyelinase activity in vitro was performed essentially as described by Chatterjee and Ghosh (1989). Briefly, monolayer cultures of cells were scraped into 5 ml H_2O with a policeman in the presence of protease inhibitors (2 μg/ml antipain, 2 μg/ml leupeptin, 2 mM PMSF, 100 KIU/ml aprotinin). The culture dish was washed with an additional 5 ml H_2O containing protease inhibitors, which was combined with the cell suspension. The cells were then placed in a nitrogen cavitation bomb (Parr Instrument Co., Moline, IL), which was maintained at 1,100 psi and 0°C for 20 min before disruption. The disrupted cells were then collected and centrifuged at 500 *g* for 5 min at 4°C and the resulting post nuclear supernatant was assayed for protein content using the Bradford reagent (Bio-Rad Laboratories, Richmond, CA) with BSA as a standard. The pellet was discarded. 10 mM C_6-NBD-SM/BSA complexes were prepared in a manner analogous to the preparation of C_6-NBD-Cer/BSA complexes (Pagano and Martin, 1988). Each reaction mixture contained 400 μl cell homogenate, 400 μl of either 250 mM sodium acetate buffer (pH 4.0–5.6) or 250 mM tris-glycine buffer (pH 6.0–8.0), 10 μl C_6-NBD-SM/BSA solution, and 8 μl of either 50 mM EDTA or 125 mM $MgCl_2$. The reaction mixtures were incubated at 37°C for 1 h and then the lipids were extracted and analyzed as described (Koval and Pagano, 1989).

Microscopy and Lysosome Labeling Procedures

Specimens were observed using a Zeiss IM-35 microscope equipped with epi-fluorescence optics and filter combinations which eliminated cross-over between NBD (or fluorescein) and rhodamine fluorescence channels. Photography and processing of photomicrographs were performed as described (Martin and Pagano, 1987).

Lysosomes were labeled by incubating cells with 600 μg/ml SRh-dextran in DME for 12 h, followed by a chase of 2 h or more at 37°C with HMEM (Ferris et al., 1987). Alternatively, lysosomes were visualized by indirect immunofluorescence using an antibody to hLAMP-2, kindly provided by Drs. Y. Cha and J. T. August (Johns Hopkins School of Medicine) (Mane et al., 1989). For double-label experiments with hLAMP-2, cells were first labeled with SRh-dextran as described above. All remaining steps were performed at room temperature. The cells were fixed in 3% paraformaldehyde-0.02% glutaraldehyde as described (Koval and Pagano, 1989), washed, and then photographed using optics appropriate for SRh fluorescence. The samples were then treated with 0.2 M glycine in H_2O for 5 min, followed by a 10-s treatment with 100% methanol at −20°C to render the cells permeable to antibodies. The cells were then washed with PBS containing 0.2% gelatin, and incubated with anti-hLAMP-2 at a 1:100 dilution in PBS-gelatin for 30 min. The cells were washed, incubated with fluorescein-conjugated goat anti-rabbit IgG at a 1:100 dilution in PBS-gelatin for 30 min, and then washed with PBS. Cells previously photographed were relocated and photographed using optics appropriate for fluorescein fluorescence.

Results

C_6-NBD-SM Labeling and Internalization

Normal and NP-A human fibroblasts incubated with 25 μM C_6-NBD-SM/DOPC (2:3; mol/mol) SUV in HMEM for 30 min at 7°C showed equivalent amounts of labeling as a result of spontaneous transfer of fluorescent SM from SUV to the cells (Table I). In some experiments, SUV used for labeling also contained 2 mol % N-SRh-DOPE, a nonexchangeable fluorescent lipid marker (Sleight and Pagano, 1984; Struck and Pagano, 1980; Struck et al., 1981) that provided a measure of SUV nonspecifically adsorbed to the cells. From these experiments we conclude that >96% of the cell-associated C_6-NBD-SM fluorescence was due to insertion of C_6-NBD-SM into the plasma membrane of both cell types.

Both normal and NP-A fibroblasts labeled with fluorescent SM at 7°C showed bright plasma membrane fluorescence (Fig. 2, *a* and *c*). As long as the labeled cells were kept at 7°C, at least 90% of the cell-associated fluorescent lipid could be removed by back-exchange (normal: 90.2 ± 12.0% (n = 3); NP-A: 90.7 ± 10.4% (n = 3)). When cells labeled at 7°C were warmed to 37°C for 10 min, internalization of fluorescent lipid was observed. As shown in Fig. 2 *b* and *d*, both normal and NP-A fibroblasts treated under these conditions had a similar distribution of intracellular vesicles containing fluorescent lipid. With increasing incubation time at 37°C, C_6-NBD-SM-labeled normal cells showed increasing Golgi apparatus fluorescence (Fig. 3 *a*), consistent with previous observations in CHO-K1 cells (Koval and Pagano, 1989). In contrast, NP-A cells showed some fluorescence in the region of the Golgi apparatus (Fig. 3 *b*), however the labeling pattern was less distinct.

Transport of C_6-NBD-SM to Lysosomes in NP-A Fibroblasts

To examine the distribution of lysosomes in human fibroblasts, cells were incubated at 37°C overnight with culture medium containing SRh-dextran, a fluorescent fluid-phase marker, followed by incubation at 37°C in HMEM alone for at least 2 h (Ferris et al., 1987). As shown in Fig. 4, this resulted in SRh-dextran accumulation in the lysosomes, as indicated by a pattern of intracellular SRh fluorescence, which showed substantial overlap with the distribution of hLAMP-2, a human lysosome-associated membrane (glyco)protein (Mane et al., 1989), as visualized by indirect immunofluorescence.

We examined the intracellular distribution of C_6-NBD-SM in NP-A and normal cells after vital staining of the lysosomes with SRh-dextran. As shown in Fig. 5, *a* and *b*, NP-A cells labeled with C_6-NBD-SM at 7°C and then incubated for 30 min at 37°C did not show fluorescent SM localized to lysosomes labeled with SRh-dextran. However, when the 37°C incubation time was increased to 2 h, lysosomes, in addition to other endocytic compartments, were labeled with C_6-NBD-SM (Fig. 5, *c* and *d*). In contrast, normal cells labeled with C_6-NBD-SM and subsequently incubated for 2 h at 37°C did not accumulate any C_6-NBD-SM in the lysosomes; rather, most of the intracellular C_6-NBD-lipid was localized to the Golgi apparatus, similar to the cells shown in Fig. 3 *a*.

Normal and NP-A cells were labeled with C_6-NBD-SM, incubated for 60 min at 37°C in HMEM, and then further incubated for 30 min at 37°C in back-exchange medium to remove C_6-NBD-lipid from endosomes and the recycling pathway (Koval and Pagano, 1989). NP-A cells treated in this manner retained intracellular C_6-NBD-SM with a punctate distribution, which colocalized with a subset of SRh-dextran labeled lysosomes (Fig. 6, *a* and *b*). However, equivalently treated normal cells showed almost exclusive Golgi apparatus fluorescence, with no observable lysosomal accumulation of C_6-NBD-lipid (Fig. 6, *c* and *d*).

Fluorescent Sphingolipid Metabolism in Human Fibroblasts

Since NP-A cells are deficient in A-SMase (Beaudet and Manschreck, 1982; Maziere et al., 1982), differences in the intracellular distribution of C_6-NBD-lipid between NP-A and normal fibroblasts were likely due to differences in the metabolism of C_6-NBD-SM. As shown in Fig. 7, both normal and NP-A fibroblasts labeled with fluorescent SM at 7°C and then incubated at 37°C showed some hydrolysis of C_6-NBD-SM to C_6-NBD-Cer, as well as production of C_6-NBD-GlcCer. To confirm that C_6-NBD-SM hydrolysis by

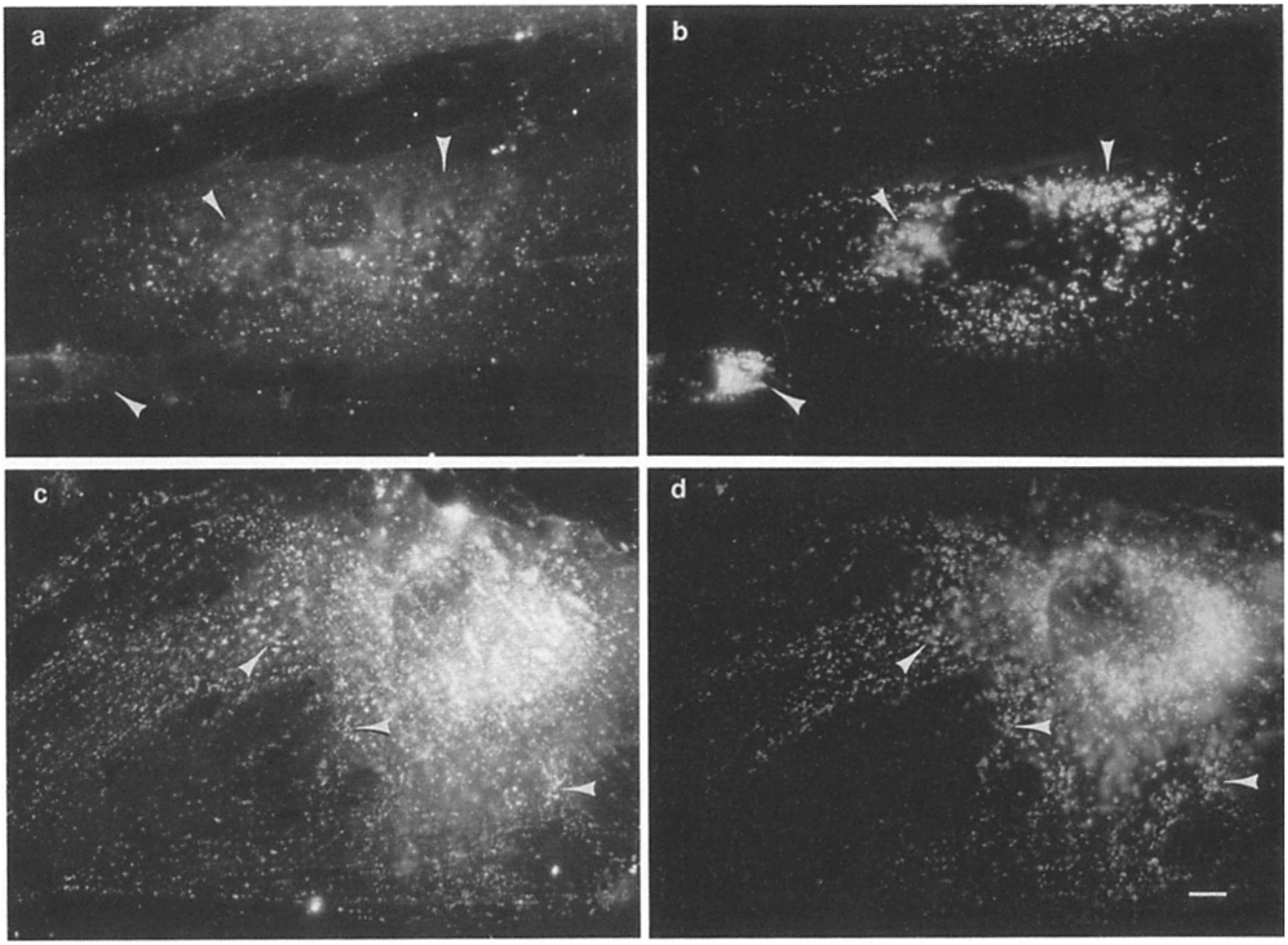

Figure 5. Transport of C_6-NBD-lipid to lysosomes by NP-A fibroblasts. NP-A human fibroblasts were labeled overnight at 37°C with SRh-dextran, washed, and incubated for 2 h at 37°C in HMEM. The cells were then labeled with SUV containing C_6-NBD-SM for 30 min at 7°C, washed, incubated in HMEM for either 30 min (*a* and *b*) or 2 h (*c* and *d*) at 37°C, washed, and then treated with back-exchange medium at 7°C. The cells were then photographed for either C_6-NBD-lipid (*a* and *c*) or SRh-dextran (*b* and *d*) fluorescence. Note that the plane of focus was selected using SRh-dextran fluorescence. Cells that were incubated for 30 min at 37°C (*a* and *b*) do not show fluorescent lipid accumulation in lysosomes (*arrowheads*). In contrast, cells incubated for 2 h at 37°C (*c* and *d*) show colocalization of fluorescent lipid and SRh-dextran labeled lysosomes. Bar, 10 μm.

NP-A fibroblasts was not due to low levels of A-SMase activity, homogenates were prepared from normal and NP-A fibroblasts and analyzed for in vitro SMase hydrolysis of fluorescent SM as a function of pH (Fig. 8). As expected, homogenates from normal cells had high levels of SMase activity at low pH. However, hydrolysis of C_6-NBD-SM by NP-A cell homogenates was Mg^{2+}-dependent, with maximum activity at pH ~7.0 and no detectable SM hydrolysis at acidic pH. The pH profile of C_6-NBD-SM hydrolysis by NP-A cell homogenates suggested that C_6-NBD-SM hydrolyzed by intact NP-A cells was due to N-SMase activity.

To determine whether intact normal and NP-A fibroblasts contained similar amounts of N-SMase, we examined the metabolism of C_6-NBD-SM in cells incubated at 19°C. It has been shown that incubation of cells at 19°C inhibits vesicular transport to the lysosomes (Dunn et al., 1980; Aulinskas et al., 1982). This was confirmed by examining cells containing lysosomes labeled with SRh-dextran, which were subsequently incubated for 2 h at 19°C in the presence of a fluid-phase marker, Lucifer Yellow. Neither normal nor NP-A cells transported Lucifer Yellow to the lysosomes during the 19°C incubation (Fig. 9, *a–d*). Further, normal or NP-A fibroblasts which were labeled with C_6-NBD-SM and subsequently incubated at 19°C for 2 h did not accumulate fluorescent C_6-NBD-SM in lysosomes (Fig. 9, *e–h*).

As shown in Table II, normal and NP-A cells incubated at 19°C hydrolyzed comparable amounts of C_6-NBD-SM. Since this represents SMase activity in the absence of transport to the lysosomes, it seems likely that normal and NP-A cells have comparable amounts of nonlysosomal SMase activity (i.e., N-SMase). Thus, the difference between the amount of C_6-NBD-SM hydrolyzed by intact normal human fibroblasts and by equivalently treated NP-A cells should reflect the amount of C_6-NBD-SM hydrolyzed by A-SMase in normal human fibroblasts. As shown in Fig. 10, the calculated time course for A-SMase activity showed a ~20–30-min lag period, followed by increasing amounts of C_6-NBD-SM hydrolysis. The lag period is likely to be related

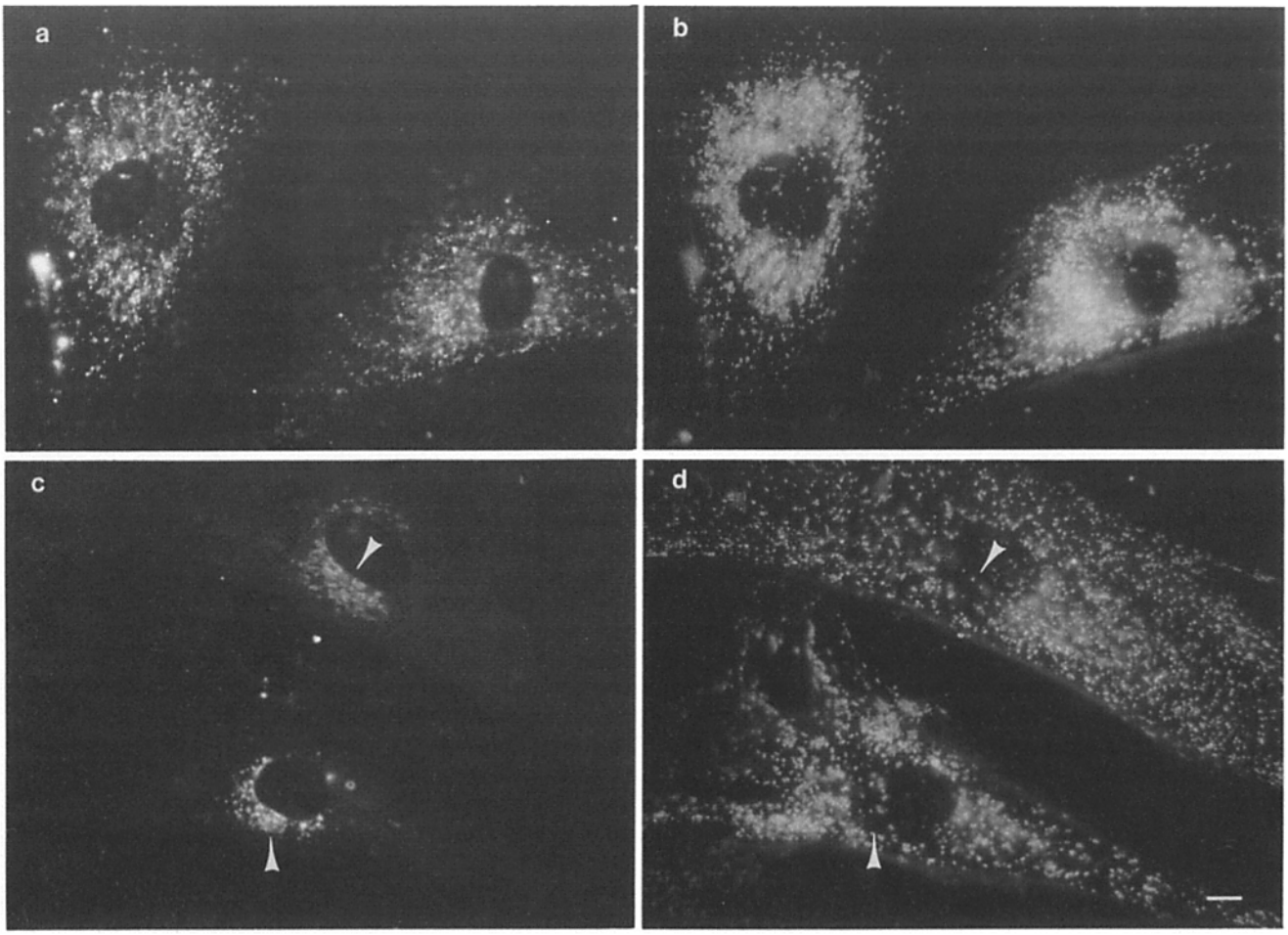

Figure 6. Comparison of C_6-NBD-SM accumulation by normal and NP-A human fibroblasts. NP-A (*a* and *b*) or normal (*c* and *d*) human fibroblasts were labeled overnight at 37°C with SRh-dextran, washed, and then incubated for 2 h at 37°C in HMEM. The cells were then labeled with SUV containing C_6-NBD-SM at 7°C for 30 min, washed, incubated for 60 min at 37°C in HMEM, followed by treatment with back-exchange medium at 7°C to remove fluorescent lipid at the plasma membrane. The cells were then further incubated in back-exchange medium at 37°C for 30 min to remove fluorescent lipid capable of recycling, washed, then photographed for either (*a* and *c*) C_6-NBD-lipid or (*b* and *d*) SRh-dextran fluorescence. Note that NP-A fibroblasts (*a* and *b*) show accumulation in lysosomes, while normal cells (*c* and *d*) show prominent labeling of the Golgi apparatus (*arrowheads*) with no detectable lysosomal labeling. Bar, 10 μm.

to the rate of lipid movement along the degradative pathway and is consistent with the lag period observed for the accumulation of C_6-NBD-SM in the lysosomes of NP-A cells (see Fig. 5, *a* and *b*).

Since normal cells did not exhibit lysosomal fluorescence, it seems likely that the rate-limiting step for A-SMase hydrolysis of C_6-NBD-SM was delivery to the lysosomes. This implies that the amount of C_6-NBD-SM hydrolyzed by A-SMase reflects the amount of C_6-NBD-SM delivered to lysosomes. Thus, from the slope of the dashed line in Fig. 10, we estimate that the rate of C_6-NBD-SM delivery to the lysosomes was 7.9 ± 2.2% of the total cell-associated C_6-NBD-lipid/h, after the lag period. By comparison, LDL particles are delivered to the lysosomes in human fibroblasts at a rate of ~68% of the total cell-associated LDL/h (Brown and Goldstein, 1979).

Quantitation of C_6-NBD-SM Endocytosis and Recycling

Fibroblasts were labeled with C_6-NBD-SM at 7°C, incubated at 37°C for increasing amounts of time, and the internalization of C_6-NBD-SM from the plasma membrane into intracellular compartments resistant to back-exchange was examined quantitatively. For normal fibroblasts, the amount of endocytosed, nonmetabolized C_6-NBD-SM reached a plateau value of ~20% of the total cell-associated C_6-NBD-lipid within 3 min, which was maintained for 2 h at 37°C (Fig. 11 *a*). In contrast, NP-A fibroblasts labeled with C_6-NBD-SM and subsequently incubated at 37°C for 2 h accumulated more intracellular, nonmetabolized C_6-NBD-SM than normal cells (normal: 19.3 ± 2.0% [n = 3]; NP-A: 35.8 ± 10.4% [n = 5]; Fig. 11 *b*). Differences between normal and NP-A cells in the amount of intracellular, nonhydrolyzed C_6-NBD-SM appeared to reflect differences in C_6-NBD-SM hydrolysis instead of differences in transport (see Discussion). Consistent with this explanation, the rate of internalization of nonmetabolized C_6-NBD-SM from the plasma membrane was comparable for both normal and NP-A fibroblasts (Fig. 11 *c*). In particular, both cell types have the same rapid initial rate of uptake.

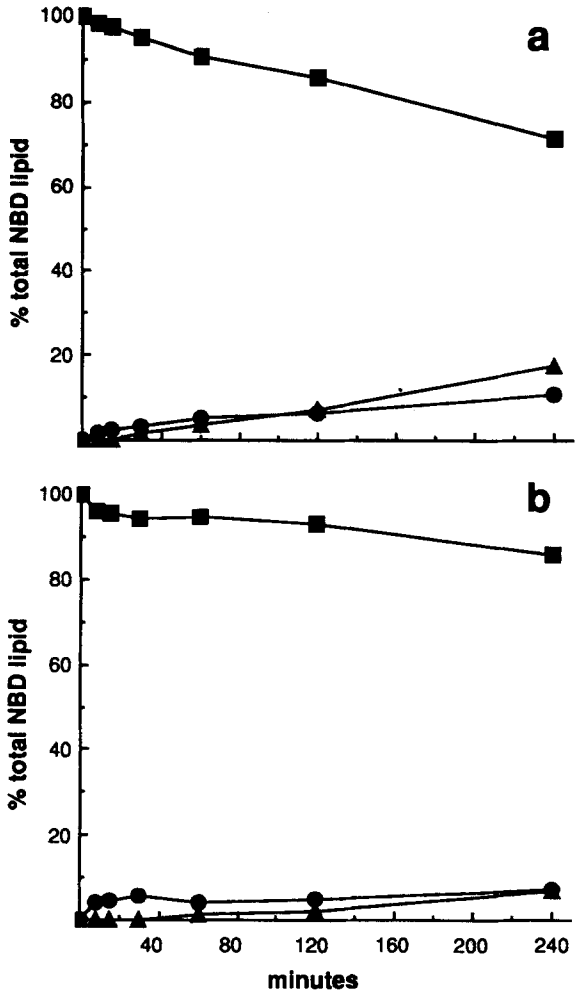

Figure 7. Metabolism of C_6-NBD-SM by normal and NP-A fibroblasts. Either normal (*a*) or NP-A (*b*) human fibroblasts were labeled with SUV containing C_6-NBD-SM for 30 min at 7°C, washed, and incubated for the indicated times at 37°C in HMEM. The cell-associated lipids were extracted, separated by TLC, and the fluorescent metabolites were measured and expressed as a percentage of total cell-associated C_6-NBD-lipid. (■) C_6-NBD-SM; (●) C_6-NBD-Cer; (▲) C_6-NBD-GlcCer. Data points are the means of triplicate measurements.

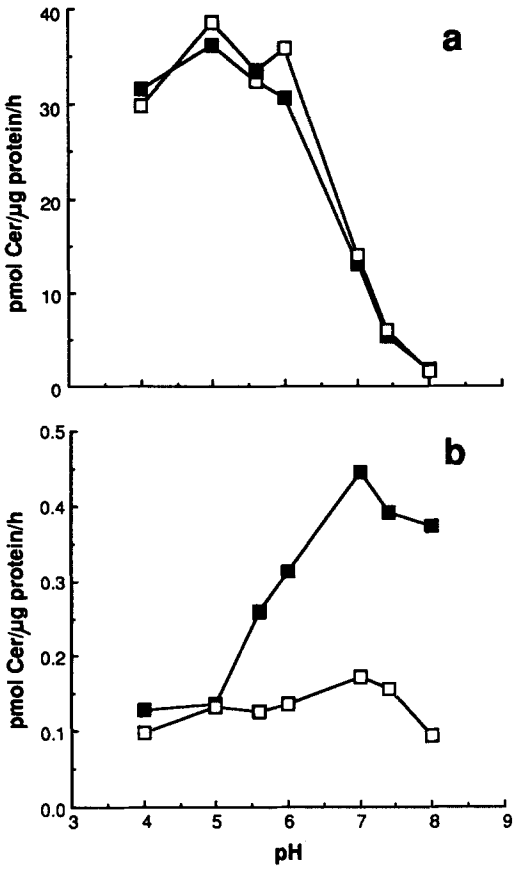

Figure 8. SMase activity of fibroblast homogenates. Either normal (*a*) or NP-A (*b*) cells were homogenized using a nitrogen cavitation bomb, and aliquots containing equal amounts of cell protein were adjusted to pH 4.5–8.0 in the presence of either Mg^{2+} or EDTA. C_6-NBD-SM was added to each aliquot and the samples were incubated at 37°C for 1 h. The lipids were then extracted, separated by TLC, and the amount of C_6-NBD-Cer formed in the presence of either Mg^{2+} (■) or EDTA (□) was measured and expressed as pmol C_6-NBD-Cer formed/μg homogenate protein per minute. Note the difference in scale between *a* and *b*. Also, SMase hydrolysis in normal cells (*a*) is not Mg^{2+} dependent, suggesting that SM hydrolysis at pH 7-7.4 in normal cells is due to A-SMase activity that is sufficient to mask N-SMase activity in these homogenates, given the level of SMase activity found in NP-A cells (*b*).

We also measured the rate of internalized fluorescent SM returned to the plasma membrane (recycling) in both cell types. Fibroblasts were labeled with C_6-NBD-SM at 7°C, washed, incubated at 37°C for 15 min, and treated with back-exchange medium at 7°C to remove fluorescent SM remaining at the plasma membrane. The cells were then further incubated at 37°C and the amount of C_6-NBD-SM returned from intracellular compartments to the plasma membrane was determined (Fig. 12). Both normal and NP-A cells showed comparable amounts of intracellular C_6-NBD-SM returned to the plasma membrane during further incubation at 37°C (Fig. 12 *c*). From this we estimate that the half-time of transport from intracellular compartments to the plasma membrane was ~5 min for both cell types, with an initial rate of 7.8 ± 1.6% C_6-NBD-SM recycled/min.

As seen in Fig. 12, after further incubation at 37°C in back-exchange medium for 1 h, NP-A fibroblasts retained more nonhydrolyzed C_6-NBD-SM in intracellular compartments (47.3 ± 19.8% [n = 3]) than did normal cells (17.6 ± 5.6% [n = 3]). This difference could be accounted for by the greater amount of C_6-NBD-SM hydrolyzed by normal fibroblasts (23.6 ± 4.9% [n = 3]). Also, the prominent Golgi apparatus labeling by normal cells observed in Fig. 6 *c* was consistent with the relatively high amounts of C_6-NBD-Cer produced by these cells, in contrast to NP-A cells, which showed less C_6-NBD-SM hydrolysis and accumulation of fluorescent SM in lysosomes (see Fig. 6 *a*).

Note that NP-A cells showed no hydrolysis of intracellular C_6-NBD-SM (Fig. 12 *b*), which was consistent with the localization of N-SMase to the cell surface. Thus, the amount of intracellular C_6-NBD-SM hydrolyzed by normal cells should directly reflect A-SMase activity, i.e., delivery to the

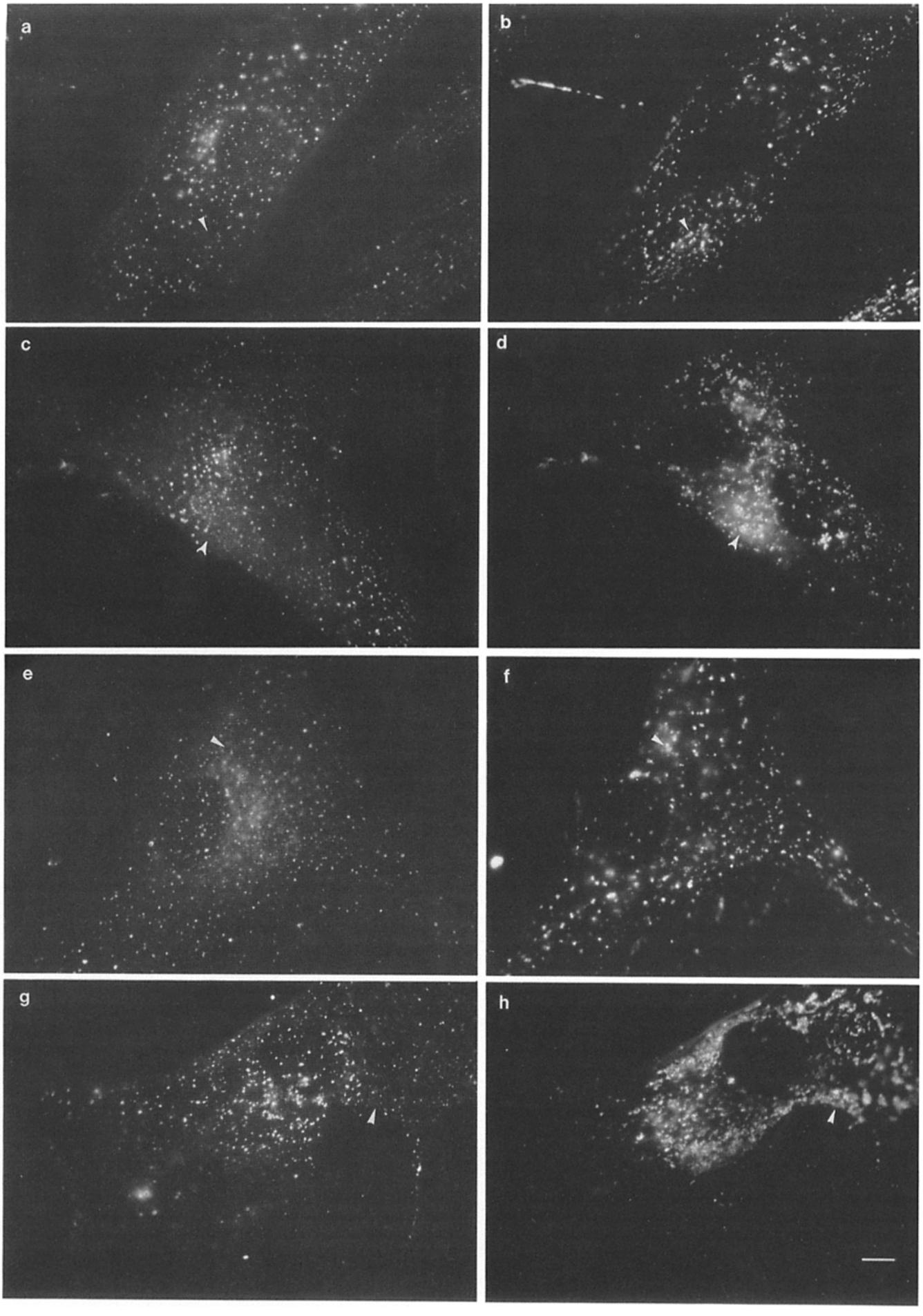
a
b
c
d
e
f
g
h

Table II. Hydrolysis of C_6-NBD-SM at 37 and 19°C

Cell type	Percent C_6-NBD-SM hydrolyzed	
	37°C	19°C
Normal	51.4 ± 8.7	24.2 ± 4.7
NP-A	19.1 ± 3.2	15.6 ± 6.3

Both normal and NP-A fibroblasts were labeled with SUV containing C_6-NBD-SM at 7°C, washed, and incubated in HMEM at either 37 or 19°C for 4 h. The cell-associated lipids were then extracted, separated by TLC, and the total C_6-NBD-SM hydrolyzed was calculated as described in the text. Values are the means ± SD of three measurements, except for NP-A cells at 19°C (six measurements).

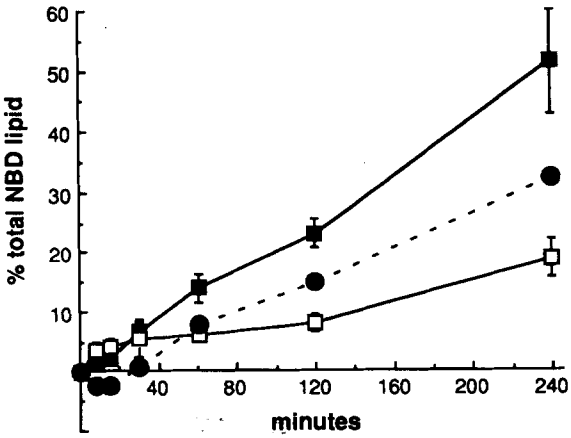

Figure 10. Differences in C_6-NBD-SM hydrolysis by fibroblasts during 37°C incubation. The total amount of C_6-NBD-SM hydrolyzed by normal (■) or NP-A (□) human fibroblasts was calculated as the sum of C_6-NBD-Cer, C_6-NBD-GlcCer, and newly synthesized C_6-NBD-SM produced by the cells as analyzed in Fig. 7. The difference in the amount of C_6-NBD-SM hydrolyzed by both cell types (●) gives a measure of the amount of fluorescent SM hydrolyzed by A-SMase in normal cells (see text). Data points are the means of triplicate measurements.

lysosomes. Further, A-SMase activity was not detected until the cells had been incubated at 37°C for a total of ~20 min (15 min incubation for internalization followed by a 5-min second incubation), consistent with the lag observed in Fig. 10. We estimate that 0.42 ± 0.06% of the intracellular C_6-NBD-SM/min was delivered to the lysosomes after this lag. From this, the rate of C_6-NBD-SM returned to the plasma membrane was determined to be 18.6 ± 4.5fold faster than the rate for C_6-NBD-SM delivery to the lysosomes.

Discussion

In this study, we compared the transport and metabolism of C_6-NBD-SM by normal human skin fibroblasts with NP-A fibroblasts. Both normal and NP-A cells incubated at 7°C with SUVs containing C_6-NBD-SM incorporated equivalent amounts of fluorescent SM into the plasma membrane (Table I), and showed similar distributions of intracellular C_6-NBD-lipid after short (10 min) incubations at 37°C (Fig. 2). In contrast to CHO-K1 fibroblasts, which accumulate intracellular vesicles containing endocytosed C_6-NBD-lipid in the perinuclear region of the cell, human fibroblasts did not collect internalized C_6-NBD-SM in a single region of the cell. Instead, vesicles containing internalized fluorescent lipid were distributed throughout the cell in both NP-A and human fibroblasts. Cell-specific differences in endosome distribution have also been observed by using both C_6-NBD-phosphatidylcholine (Sleight and Abanto, 1989) and fluorescent conjugates of transferrin (Salzman and Maxfield, 1988) as markers for endocytosis.

Rates of endocytosis (Fig. 11 *c*) and recycling (Fig. 12 *c*) were comparable for both cell types. However, NP-A fibroblasts differed from normal cells in the amount of intracellular, nonmetabolized C_6-NBD-SM accumulated during 37°C incubations. This observation can be interpreted in light of the accumulation of C_6-NBD-SM in lysosomes by NP-A cells. For normal cells, the intracellular pool of nonmetabolized C_6-NBD-SM is increased by endocytosis (Fig. 1, pathway *I*) and decreased by return of nonmetabolized C_6-NBD-SM to the plasma membrane (pathway *II*) and by transport to the lysosomes (pathway *III*), followed by hydrolysis of C_6-NBD-SM to C_6-NBD-Cer by A-SMase (Fig. 1, *broken lines*). In contrast, NP-A fibroblasts do not hydrolyze C_6-NBD-SM at the lysosomes. Therefore, delivery to the lysosomes redistributes, but does not decrease, the intracellular pool of nonmetabolized C_6-NBD-SM. Thus, if rates of endocytosis, recycling, and delivery to the lysosomes are comparable for both cell types, then the amount of C_6-NBD-SM internalized by NP-A fibroblasts should be equivalent to the sum of the amount of C_6-NBD-SM hydrolyzed by A-SMase and the amount of nonmetabolized, intracellular C_6-NBD-SM present in normal human fibroblasts. As shown in Table III, this appears to be the case.

Both normal and NP-A fibroblasts recycled plasma membrane lipid at rates similar to the rate of LDL receptor recycling in human fibroblasts, where receptors recycle between intracellular compartments and the plasma membrane once every 10 min (Brown and Goldstein, 1979; Goldstein et al., 1985). The rate for C_6-NBD-SM recycling to the plasma membrane was ~18–19 times faster than the rate for C_6-

Figure 9. Inhibition of transport to lysosomes in normal and NP-A cells incubated at 19°C. For all cases, cells were first labeled overnight at 37°C with SRh-dextran, washed, and then incubated for 2 h in HMEM at 37°C. (*a–d*) Normal (*a* and *b*) or NP-A (*c* and *d*) cells were subsequently incubated for 2 h at 19°C in HMEM containing the fluorescent fluid phase marker, Lucifer Yellow, washed, and then photographed for Lucifer Yellow (*a* and *c*) or SRh-dextran (*b* and *d*) fluorescence. Neither normal nor NP-A cells accumulated Lucifer Yellow in lysosomes (*arrowheads*) at 19°C. (*e–h*) Normal (*e* and *f*) or NP-A (*g* and *h*) cells were labeled with SUV containing C_6-NBD-SM for 30 min at 7°C, washed, and incubated for 2 h at 19°C, followed by back-exchange at 7°C. The cells were then washed and photographed for NBD (*e* and *g*) and SRh-dextran (*f* and *h*) fluorescence. Note the lack of lysosomal labeling (*arrowheads*) by C_6-NBD-SM in NP-A fibroblasts at 19°C, in contrast to the accumulation of C_6-NBD-SM in lysosomes observed at 37°C (see Fig. 5, *c* and *d*). Bar, 10 μm.

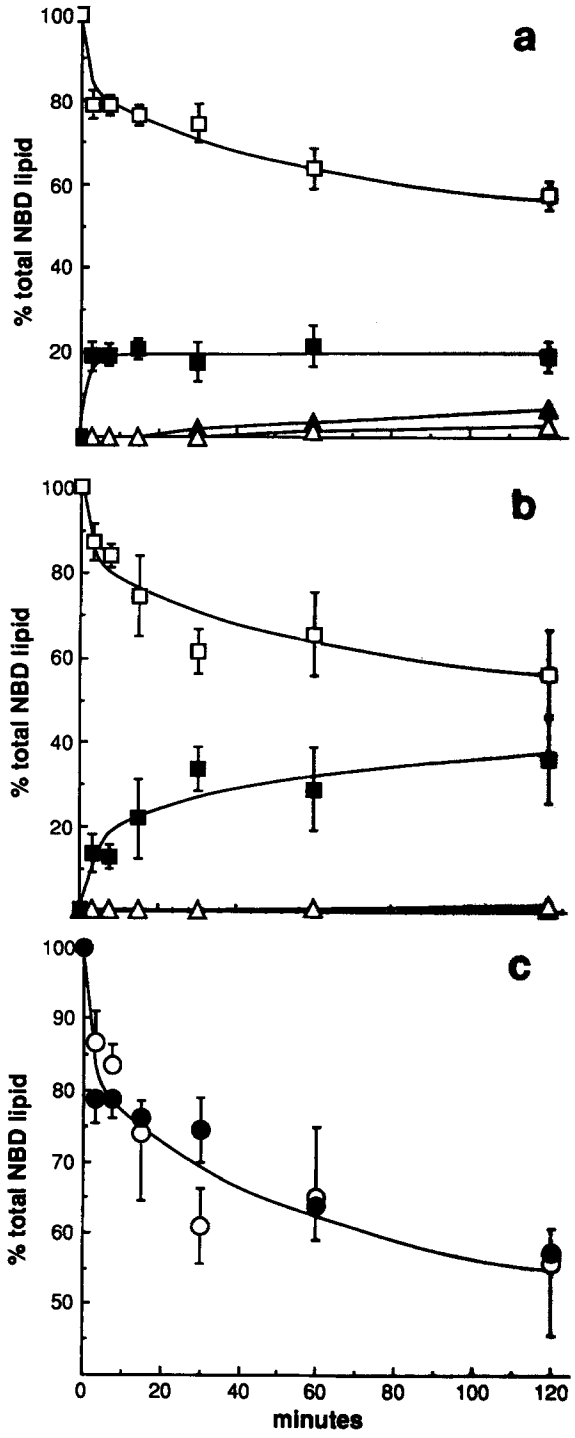

Figure 11. Quantitative analysis of C_6-NBD-SM internalization upon 37°C incubation. (*a* and *b*) Normal (*a*) or NP-A (*b*) human fibroblasts were labeled with SUV containing C_6-NBD-SM for 30 min at 7°C, washed, incubated at 37°C in HMEM for the indicated amount of time, and then harvested either immediately, or, in parallel experiments, after treatment with back-exchange medium at 7°C to remove C_6-NBD-SM remaining at the plasma membrane. The cell-associated lipids were extracted and analyzed by TLC as described in the text. The amount of back-exchangeable C_6-NBD-SM was calculated using Eq. 1 (see Materials and Methods) and all values are expressed as a percentage of total cell-associated C_6-NBD-lipid. The amounts of newly synthesized C_6-NBD-SM and nonmetabolized C_6-NBD-SM were calculated by Eqs. 2 and 3, respectively (see Materials and Methods). (□) Nonmetabolized C_6-NBD-SM at the plasma membrane; (■) intracellular nonmetabolized C_6-NBD-SM; (△) newly synthesized C_6-NBD-SM at the plasma membrane; (▲) intracellular newly synthesized C_6-NBD-SM. Data points are the means of either three (*a*) or five (*b*) measurements and are expressed as percentages of the total cell-associated NBD lipid. (*c*) Comparison of the amount of nonmetabolized C_6-NBD-SM remaining at the plasma membrane for normal (○) and NP-A cells (●) showing that uptake of C_6-NBD-SM is similar for both cell types. Data points are the means ± SD.

Table III. Comparison of C_6-NBD-SM Internalization for Normal and NP-A Cells

	Percent of total C_6-NBD-lipid			
	Normal			NP-A
Hours	Intracellular nonmetabolized C_6-NBD-SM	C_6-NBD-SM hydrolyzed by A-SMase	Sum	Intracellular nonmetabolized C_6-NBD-SM
1	22.7 ± 5.0	9.2 ± 2.4	31.9 ± 5.5	28.8 ± 18.8
2	19.3 ± 2.0	17.7 ± 3.7	37.0 ± 4.1	35.8 ± 10.4

Values for intracellular, nonmetabolized C_6-NBD-SM for normal cells are from Fig. 11 *a*; values for C_6-NBD-SM hydrolyzed by A-SMase are from Fig. 10; values for intracellular, nonmetabolized C_6-NBD-SM for NP-A cells are from Fig. 11 *b*. Cells were labeled with SUV containing C_6-NBD-SM at 7°C, followed by incubation for 1 or 2 h at 37°C. Sum is defined as the sum of intracellular, nonmetabolized C_6-NBD-SM and C_6-NBD-SM hydrolyzed by A-SMase for normal cells. See text for details.

NBD-SM delivery to lysosomes, after the lag period. We believe that this ratio reflects the relative amount of C_6-NBD-SM sorted between the recycling and degradative pathways. Since there was a 20–30-min lag before detectable A-SMase hydrolysis, fluorescent SM destined for lysosomal hydrolysis was either sequestered into a nonrecycling portion of the sorting endosome or delivered to some other prelysosomal compartments that lack A-SM. If sorting of C_6-NBD-SM to these compartments was faster than lipid movement along the degradative pathway, then the pool of nonmetabolized, intracellular C_6-NBD-SM, shown in Fig. 11, should slowly increase during a 37°C incubation as a result of accumulation in prelysosomal compartments. However, after the rapid loading of endosomal and recycling compartments, levels of nonmetabolized, intracellular C_6-NBD-SM remain constant in normal cells. Similar results were previously observed for CHO-K1 cells (Koval and Pagano, 1989). This suggests that C_6-NBD-SM sorting between the plasma membrane recycling and degradative pathways is the rate limiting step in commitment of endocytosed C_6-NBD-SM for transport to lysosomes.

It has been determined that 60–90% of the sorting endosome membrane of baby hamster kidney fibroblasts is organized into tubules, which are believed to be involved in plasma membrane recycling (Marsh et al., 1986; Griffiths et al., 1989). Although similar measurements have not been made on human skin fibroblasts, it appears that the sorting of endocytosed C_6-NBD-SM reflects the relative amount of sorting endosome membrane transported along the recycling and degradative pathways, since C_6-NBD-SM should be free to diffuse throughout the entire sorting endosome membrane. This is also consistent with the results of Dunn et al.

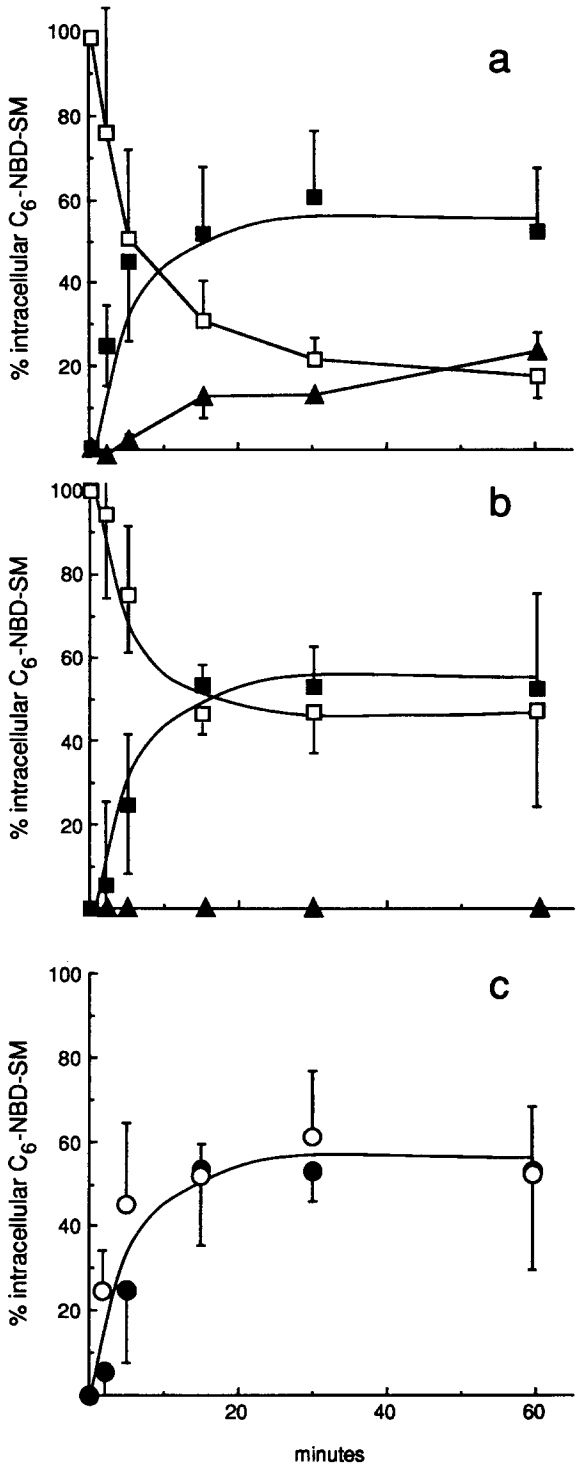

Figure 12. Quantitation of C_6-NBD-SM recycling to the plasma membrane. (*a* and *b*) Normal (*a*) or NP-A (*b*) human fibroblasts were labeled with SUV containing C_6-NBD-SM at 7°C for 30 min, washed, incubated at 37°C for 15 min, and treated with back-exchange medium at 7°C to remove C_6-NBD-SM remaining at the plasma membrane. The cells were then further incubated for the indicated amount of time at 37°C in either HMEM or back-exchange medium, washed, and the cell-associated lipids were extracted and analyzed by TLC (see Materials and Methods). The amount of nonmetabolized C_6-NBD-SM was calculated using Eqs. 1–3, while the amount of C_6-NBD-SM hydrolyzed was calculated as described in the legend of Fig. 11. (■) Nonmetabolized C_6-NBD-SM returned to the plasma membrane; (□) intracellular nonmetabolized C_6-NBD-SM; (▲) total cell-associated C_6-NBD-SM hydrolyzed. Data points are the means of triplicate measurements expressed as percentages of the total cell-associated lipid. (*c*) Comparison of the amounts of intracellular nonmetabolized C_6-NBD-SM returned to the plasma membrane by normal (○) and NP-A cells (●) showing that recycling of C_6-NBD-SM is similar for both cell types. Data points are the means ± SD of triplicate measurements expressed as percentages of the total initial cell-associated intracellular C_6-NBD-SM.

(1989), where sorting of endocytic traffic can be modeled by assuming that vesicles recycled to the plasma membrane from sorting endosomes have a high surface to volume ratio.

Although "reverse-flow" of proteins from lysosomes to other compartments (e.g., plasma membrane) has been described (Lippincott-Schwartz and Fambrough, 1987), it is not certain whether this represents a universal mechanism for transport of material out of lysosomes. As depicted in Fig. 1, C_6-NBD-SM hydrolysis to C_6-NBD-Cer is required for rapid depletion of C_6-NBD-SM from the lysosomes. Note that further hydrolysis of C_6-NBD-Cer to C_6-NBD-fatty acid and sphingosine did not occur in this and other studies (Lipsky and Pagano, 1983, 1985*a*). We speculate that transport of C_6-NBD-Cer from lysosomes to the Golgi apparatus might reflect a pathway for endogenous Cer transport. However, since C_6-NBD-Cer is capable of spontaneous transbilayer movement and transfer between membranes by monomer diffusion (Pagano, 1989), we cannot infer whether facilitated movement of endogenous Cer produced at the lysosomes might occur. To address this issue, it should be possible to examine the intracellular transport and metabolism of fluorescent SM analogues containing long chain fatty acids. The resulting Cer produced by hydrolysis of long chain fluorescent SM would not spontaneously transfer between membranes and could only exit rapidly from lysosomes by a facilitated transport pathway.

We are grateful to Drs. Y. Cha and J. T. August for their gift of anti-hLAMP2. We thank Ms. O. Martin, Mr. A. Ting, Dr. A. Futerman, Dr. P. Hoffmann-Bleihauer, and Dr. A. Rosenwald for critical reading of the manuscript.

This work was supported by United States Public Health Service grant R37 GM22942.

Received for publication 6 February 1990 and in revised form 25 April 1990.

References

Aulinskas T. H., G. A. Coetzee, W. Gevers, and D. R. van der Westhuyzen. 1982. Evidence that recycling of low density lipoprotein receptors does not depend on delivery of receptors to lysosomes. *Biochem. Biophys. Res. Commun.* 107:1551–1558.

Beaudet, A. L., and A. A. Manschreck. 1982. Metabolism of sphingomyelin by intact cultured fibroblasts: differentiation of Niemann-Pick disease, types A and B. *Biochem. Biophys. Res. Commun.* 105:14–19.

Bligh, E. G., and W. J. Dyer. 1959. A rapid method of total lipid extraction and purification. *Can. J. Biochem. Physiol.* 37:911–917.

Brown, M. S., and J. L. Goldstein. 1979. Receptor-mediated endocytosis: insights from the lipoprotein receptor system. *Proc. Natl. Acad. Sci. USA.* 76:3330–3337.

Chatterjee, S., and N. Ghosh. 1989. Neutral sphingomyelinase from human urine. Purification and preparation of monospecific antibodies. *J. Biol. Chem.* 264:12554–12561.

Dunn, K. W., T. E. McGraw, and F. R. Maxfield. 1989. Iterative fractionation of recycling receptors from lysosomally destined ligands in an early sorting endosome. *J. Cell Biol.* 109:3303–3314.

Dunn, W. A., A. L. Hubbard, and N. N. Aronson, Jr. 1980. Low temperature

selectively inhibits fusion between pinocytic vesicles and lysosomes during heterophagy of ^{125}-asialofetuin by the perfused rat liver. *J. Biol. Chem.* 255:5971–5978.

Ferris, A. L., J. C. Brown, R. D. Park, and B. Storrie. 1987. Chinese hamster ovary cell lysosomes rapidly exchange contents. *J. Cell Biol.* 105:2703–2712.

Geuze, H. J., J. W. Slot, G. J. A. M. Strous, H. F. Lodish, and A. L. Schwartz. 1983. Intracellular site of asialoglycoprotein receptor-ligand uncoupling: double-label immunoelectron microscopy during receptor-mediated endocytosis. *Cell.* 32:277–287.

Geuze, H. J., J. W. Slot, and A. L. Schwartz. 1987. Membranes of sorting organelles display lateral heterogeneity in receptor distribution. *J. Cell Biol.* 104:1715–1723.

Goldstein, J. L., M. S. Brown, R. G. W. Anderson, D. W. Russell, and W. J. Schneider. 1985. Receptor-mediated endocytosis: concepts emerging from the LDL receptor system. *Annu. Rev. Cell Biol.* 1:1–39.

Griffiths, G., R. Back, and M. Marsh. 1989. A quantitative analysis of the endocytic pathway in baby hamster kidney cells. *J. Cell Biol.* 109:2703–2720.

Hope, M. J., M. B. Bally, G. Webb, and P. R. Cullis. 1985. Production of large unilammellar vesicles by a rapid extrusion procedure. Characterization of size distribution, trapped volume and ability to maintain a membrane potential. *Biochem. Biophys. Acta.* 812:55–65.

Hubbard, A. L. 1989. Endocytosis. *Curr. Op. Cell Biol.* 1:675–683.

Koval, M., and R. E. Pagano. 1989. Lipid recycling between the plasma membrane and intracellular compartments: transport and metabolism of fluorescent sphingomyelin analogues in cultured fibroblasts. *J. Cell Biol.* 108: 2169–2181.

Kremer, J. M. H., M. W. J. v. d. Esker, C. Pathmamanoharan, and P. H. Wiersema. 1977. Vesicles of variable diameter prepared by a modified injection method. *Biochemistry.* 16:3932–3935.

Kudoh, T., M. A. Velkoff, and D. A. Wenger. 1983. Uptake and metabolism of radioactively labeled sphingomyelin in cultured skin fibroblasts from controls and patients with Niemann-Pick disease and other lysosomal storage diseases. *Biochim. Biophys. Acta.* 918:754:82–92.

Labarca, C., and K. Paigen. 1980. A simple, rapid and sensitive DNA assay procedure. *Anal. Biochem.* 102:344–352.

Levade, T., and S. Gatt. 1987. Uptake and intracellular degradation of fluorescent sphingomyelin by fibroblasts from normal individuals and a patient with Niemann-Pick disease. *Biochim. Biophys. Acta.* 250–259.

Linderman, J. L., and D. A. Lauffenburger. 1988. Analysis of intracellular receptor/ligand sorting in endosomes. *J. Theor. Biol.* 132:203–245.

Lippincott-Schwartz, J., and D. M. Fambrough. 1987. Cycling of the integral membrane protein, LEP100, between plasma membrane and lysosomes: kinetic and morphological analysis. *Cell.* 49:669–685.

Lipsky, N. G., and R. E. Pagano. 1983. Sphingolipid metabolism in cultured fibroblasts: microscopic and biochemical studies employing a fluorescent ceramide analogue. *Proc. Natl. Acad. Sci. USA.* 80:2608–2612.

Lipsky, N. G., and R. E. Pagano. 1985*a*. Intracellular translocation of fluorescent sphingolipids in cultured fibroblasts: endogenously synthesized sphingomyelin and glucosylcerebroside analogues pass through the Golgi apparatus en route to the plasma membrane. *J. Cell Biol.* 100:27–34.

Lipsky, N. G., and R. E. Pagano. 1985*b*. A vital stain for the Golgi apparatus. *Science (Wash. DC).* 228:745–747.

Mane, S. M., L. Marzella, D. P. Bainton, V. K. Holt, Y. Cha, J. E. K. Hildreth, and J. T. August. 1989. Purification and characterization of human lysosomal membrane glycoproteins. *Arch. Biochem. Biophys.* 268:360–378.

Marsh, M., G. Griffiths, G. E. Dean, I. Mellman, and A. Helenius. 1986. Three-dimensional structure of endosomes in BHK-21 cells. *Proc. Natl. Acad. Sci. USA.* 83:2899–2903.

Martin, O. C., and R. E. Pagano. 1987. Transbilayer movement of fluorescent analogs of phosphatidylserine and phosphatidylethanolamine at the plasma membrane of cultured cells. *J. Biol. Chem.* 262:5890–5898.

Maziere, J. C., C. Maziere, L. Mora, J. D. Routier, and J. Polonovski. 1982. In situ degradation of sphingomyelin by cultured fibroblasts and fibroblasts from patients with Niemann-Pick disease type A and C. *Biochem. Biophys. Res. Commun.* 108:1101–1106.

Pagano, R. E. 1989. A fluorescent derivative of ceramide: physical properties and use in studying the Golgi apparatus of animal cells. *Methods Cell Biol.* 29:75–85.

Pagano, R. E. 1990. The Golgi apparatus: insights from lipid biochemistry. *Biochem. Soc. Trans.* 18:361–366.

Pagano, R. E., and O. C. Martin. 1988. A series of fluorescent *N*-(acyl)-sphingosines: synthesis, physical properties, and studies in cultured cells. *Biochemistry.* 27:4439–4445.

Pagano, R. E., M. A. Sepanski, and O. C. Martin. 1989. Molecular trapping of a fluorescent ceramide analogue at the Golgi apparatus of fixed cells: interaction with endogenous lipids provides a *trans*-Golgi marker for both light and electron microscopy. *J. Cell Biol.* 109:2067–2079.

Rome, H. L. 1985. Curling receptors. *Trends Biochem. Sci.* 10:151.

Rouser, B., A. N. Siakotos, and S. Fleischer. 1966. Quantitative analysis of phospholipids by thin-layer chromatography and phosphorous analysis of spots. *Lipids.* 1:85–86.

Salzman, N. H., and F. R. Maxfield. 1988. Intracellular fusion of sequentially formed endocytic compartments. *J. Cell Biol.* 106:1083–1091.

Sleight, R. G., and M. N. Abanto. 1989. Differences in intracellular transport of a fluorescent phosphatidylcholine analog in established cell lines. *J. Cell Sci.* 63:363–374.

Sleight, R. G., and R. E. Pagano. 1984. Transport of a fluorescent phosphatidylcholine analog from the plasma membrane to the Golgi apparatus. *J. Cell Biol.* 99:742–751.

Spence, M. W., J. T. R. Clarke, and H. W. Cook. 1983. Pathways of sphingomyelin metabolism in cultured fibroblasts from normal and sphingomyelin lipidosis subjects. *J. Biol. Chem.* 258:8595–8600.

Struck, D. K., and R. E. Pagano. 1980. Insertion of fluorescent phospholipids into the plasma membrane of a mammalian cell. *J. Biol. Chem.* 255:5404–5410.

Struck, D. K., D. Hoekstra, and R. E. Pagano. 1981. Use of resonance energy transfer to monitor membrane fusion. *Biochemistry.* 20:4093–4099.

Sutrina, S. L., and W. W. Chen. 1984. Lysosomal involvement in cellular turnover of plasma membrane sphingomyelin. *Biochim. Biophys. Acta.* 793: 169–179.

Uster, P. S., and R. E. Pagano. 1986.Resonance energy transfer microscopy: observations of membrane-bound fluorescent probes in model membranes and in living cells. *J. Cell Biol.* 103:1221–1234.

van Meer, G., E. H. K. Stelzer, W. Wijnaendts-van-Resandt, and K. Simons. 1987. Sorting of sphingolipids in epithelial (Madin-Darby canine kidney) cells. *J. Cell Biol.* 105:1623–1635.

Wileman, T., C. Harding, and P. Stahl. 1985. Receptor-mediated endocytosis. *Biochem. J.* 232:1–14.